

ON THE POST-PEAK DUCTILITY OF SHEAR-CRITICAL BEAMS

Frank J. Vecchio

SYNOPSIS:

Code procedures for the seismic design of reinforced concrete structures are increasingly incorporating performance-based criteria, with 'push-over' analyses becoming an accepted means of demonstrating sufficient energy-absorbing capacity. Hence, in concrete frame structures containing shear-critical structural elements, the post-peak load-deformation response of these members becomes of practical importance.

A series of shear-critical beams was tested recently, patterned after the classic set of beams tested by Bresler and Scordelis forty years ago. In the current tests, particular attention was paid to capturing the post-peak response. The details and results of these beams are presented, providing data useful in testing and calibrating analytical procedures.

Nonlinear finite element analyses were undertaken to determine current ability to accurately model post-peak ductility in shear-critical members. Results indicate that current procedures are of marginally acceptable accuracy, and that further developmental work is warranted.

A case study, involving a large concrete frame structure built in a high seismic region and containing shear-deficient members, is discussed. This case underscores the importance of accurately calculating the post-peak ductility of shear-critical beams.

KEY WORDS:

analysis, beams, ductility, finite element, push-over, reinforced concrete, seismic design, shear, tests

Frank J. Vecchio, professor, has been with the Dept. of Civil Engineering, University of Toronto since 1985. His interests relate to nonlinear analysis of reinforced concrete, constitutive modelling, assessment of structural integrity, analysis of repaired and rehabilitated structures, and forensic assessment of distressed or failed structures. Professor Vecchio is currently deputy chair of fib Commission 4 – Modelling of Structural Behaviour and Design, and is a member of ACI-ASCE Committee 445 – Finite Element Analysis of Reinforced Concrete, and ACI Committee 441 – Columns

INTRODUCTION

In the still-evolving field of nonlinear finite element analysis of reinforced concrete structures, the pioneering work undertaken by Scordelis in the early 1960s was fundamental in defining the concepts and approaches generally followed by the research community since. Among Professor Scordelis' many contributions was a seminal paper describing the testing of a series of twelve reinforced concrete beams (Bresler and Scordelis, 1963), aimed primarily at investigating shear-critical behaviour but also at providing data to support finite element development work. The beams tested covered a wide range of reinforcement and span conditions, and hence a range of influencing factors and failure modes. They have since been used extensively as benchmark data for calibrating or verifying finite element models for reinforced concrete, particularly for modelling of beams critical in shear.

A test program was recently undertaken at the University of Toronto to recreate, as much as possible, the Bresler-Scordelis test series. There were several objectives in doing so. One aim was to determine the extent of repeatability of the test results, particularly with respect to load capacity and failure mode, given that there would be some unavoidable differences in construction, material properties, and testing procedures. Another goal was to obtain information on post-peak response; the load-deflection response reported for the Bresler-Scordelis beams abruptly terminated at the peak loads. New insights into the behaviour of these beams, such as the nature of important influencing factors and critical behaviour mechanisms, would also hopefully emerge from new first-hand test observations. Finally, insights were sought into critical factors affecting accuracy in finite element modelling of these beams, with hopefully some indication emerging regarding current ability to numerically simulate post-peak response.

The ability to accurately model the post-peak ductility response of shear-critical beams is becoming of increasing importance as modern design codes move toward performance-based criteria. In particular, in satisfying requirements for the seismic design of special moment-resisting frames, one option is to perform a monotonic 'push-over' analysis and demonstrate that the structure can withstand a certain degree of lateral displacement before losing stability. In situations where beams or columns within the structure are shear-critical, a shear failure may occur within a member before it is able to develop full flexural capacity and hence before it can undergo large rotational deformation. Here, an accurate modelling of the post-peak shear response is critical if the

push-over analysis is to provide a realistic assessment of the energy-dissipation capacity of the structure.

In this paper, the details and results of the Toronto test beams are presented and discussed. Also discussed are the results of finite element simulations, particularly with respect to the accuracy of the calculated post-peak responses. Modelling factors and behaviour mechanisms influencing the observed and calculated responses are examined. Finally, the relevance of these issues is highlighted in the details of a case study.

BRESLER-SCORDELIS TEST BEAMS

The twelve beams tested by Bresler and Scordelis consisted of four series of three beams; each series differed in amount of longitudinal reinforcement, amount of shear reinforcement, span length, cross section dimensions, and concrete strength. All beams were of rectangular cross section with the same overall depth. Shear reinforcement, where provided, was in the form of closed stirrups; shear reinforcement ratios ranged from 0.0 % to 0.2 %. To prevent bond failure due to possibly insufficient anchorage, the bottom longitudinal reinforcement was extended through the ends of the beam and anchored to 35-mm steel end-plates via special anchor nuts. It should be noted that heavy amounts of flexural reinforcement were used in attempting to make the beams shear-critical. All beams were subjected to monotonic centre-point loading, with a force-controlled loading procedure employed. Additional details regarding the test specimens and test results are provided by Bresler and Scordelis (1963).

DETAILS OF TORONTO TEST BEAMS

The twelve Toronto beams were nominally identical to the Bresler-Scordelis beams in terms of cross section dimensions, amount and strength of reinforcement provided, and concrete compressive strength. Also, details relating to the longitudinal reinforcement anchor plates, the loading plates, and the support plates were preserved. Unlike the Bresler-Scordelis beams, however, a displacement-controlled loading system was used, so that post-peak response could be observed and monitored.

Cross section details are given in Figure 1, and the beam profiles are shown in Figure 2. Table 1 provides additional relevant details. [To facilitate comparisons, the specimen names given to the Toronto beams are the same as those for the corresponding Bresler-Scordelis beams except prefixed with VS-.] Due to the unavailability of adequate amounts of the imperial-sized bars, metric-sized bars were used instead. M25 and M30 bars ($A_s = 500 \text{ mm}^2$ and 700 mm^2 , respectively) were used in various combinations to obtain roughly the same reinforcement ratios as in the Bresler-Scordelis beams. Similarly, M10 bars ($A_s = 100 \text{ mm}^2$) were used for the compression reinforcement, and D4 and D5 deformed bars ($A_s = 25.7 \text{ mm}^2$ and 32.2 mm^2 , respectively) were used for the stirrups. As with the original beams, the bottom longitudinal bars were extended past the ends of the beam and anchored to a 25-mm-thick end-plates, in this case by welding. Material properties of the concrete (at time of beam test), longitudinal reinforcement and

shear reinforcement for the Toronto beams are summarized in Table 2. The maximum aggregate size was 20 mm (3/4-inch).

The test set-up used to perform the Toronto experiments is schematically shown in Figure 3. Note that a servo-controlled MTS 2700 kN universal testing machine was used to apply centre-point loading. As with the Bresler-Scordelis beams, the loads were initially applied in 40 kN increments per load stage. Near ultimate, loading was altered to displacement control, allowing the continuation of the tests into the post-peak load regimes. The specimens were instrumented for electronic monitoring of midspan- and end-deflections, and for strains in the longitudinal reinforcement in the midspan regions. Note that the Toronto beams were not initially pre-loaded and unloaded, as was done with the Bresler-Scordelis beams. Also note that the average age at testing was considerably greater; approximately 38 days for the 4.1 m beams, 51 days for the 5.0 m beams, and 127 days for the 6.8 m beams. [The Bresler-Scordelis beams were each tested at an age of 13 days.]

While attempts were made to match the Bresler-Scordelis beams as much as possible in terms of dimensions, reinforcement details and material strengths, some unavoidable variations arose. Table 3 compares the differences in reinforcement amounts; generally, the reinforcement ratios are well matched in most cases. With respect to the shear reinforcement, although the amounts of reinforcement are identical, the yield strengths of the stirrup steel are considerably different and will have some influence on the results. [Differences in the yield strength of the longitudinal reinforcement are largely irrelevant since yielding of the longitudinal steel was not a major factor in most tests.] Note too that there are some appreciable differences in concrete strengths between corresponding BS- and VS-beams, despite best efforts to match them.

RESULTS OF TORONTO TESTS

The Bresler-Scordelis beams were characterized by three different modes of damage: diagonal-tension (D-T), shear-compression (V-C), and flexure-compression (F-C). The diagonal tension failures were observed in all beams containing no shear reinforcement. The shear-compression mode was dominant in the short- and intermediate-span beams containing web reinforcement, and the flexure-compression mode prevailed in the long-span beams containing web reinforcement. The Toronto beams exhibited responses similar, in most respects, to the corresponding Bresler-Scordelis beams.

In the Toronto beams containing no shear reinforcement (i.e., OA1, OA2 and OA3), behaviour was characterized by sudden failure resulting from diagonal tension cracking. Shortly after its formation, the critical diagonal crack propagated rapidly down to the depth of the top-most layer of tension reinforcement, and then continued as a large horizontal crack to the end of the beam (e.g., see Figure 4 (a)). Failure was sudden and brittle, with no ductility in the load-deformation response beyond the peak load.

In the beams of short and intermediate length containing web reinforcement (i.e., A1, A2, B1, B2, C1, C2), behaviour could be characterized as shear-flexural in nature. These beams exhibited severe diagonal tension cracks during later load stages, as shown in Figure 4(b) for Beam VS-A1 for example, with crack widths as large as 2.0 mm. However, both the initial distress and final failure occurred by crushing of concrete in the compression zone; there was no accompanying splitting along the tension reinforcement. Flexural cracks in the midspan regions were relatively insignificant, with crack widths generally in the range of 0.5 to 1.0 mm. Most notable was the crushing of concrete beneath and adjacent to the loading plate, occurring before any shear distress was prevalent. These beams generally exhibited a small measure of ductility at the peak-load level before a sudden drop-off in load capacity occurred.

The long-span beams (i.e., A3, B3 and C3), generally exhibited a flexure-compression failure. Again, failure was induced by crushing of the concrete in the compression zone, notably appearing first under the loading plate. Unlike the intermediate-length beams, diagonal tension cracking was minor if present at all. The flexure crack widths were, in some cases, as high as 1.5 mm. Pronounced yielding of the tension reinforcement was not detected in any beam, although it appeared imminent in some cases (e.g. Beams A3 and B3). The load-deformation response of these beams demonstrated a fair measure of post-peak ductility.

The observed load-deformation responses for the twelve test beams are given in Figure 5.

COMPARISON OF TEST RESULTS

All twelve Toronto beams experienced a failure mode nominally similar to the one observed in the corresponding Bresler-Scordelis beam. However, in comparing the load-deformation responses for each pair of specimens, the Toronto beams generally exhibited lower stiffness in the ascending response, and greater deformation at ultimate. This was observed despite deformation-control at each load step, which would have minimized short-term creep effects, and despite the slightly higher concrete strengths in the Toronto beams. The Bresler-Scordelis beams did contain approximately 4% more flexural tension reinforcement, on average, explaining to some extent the greater stiffnesses. Also, pre-loading of the Bresler-Scordelis beams may have had some influence.

Compared in Figure 6(a) are the ultimate load capacities of the two set of beams. The Toronto beams consistently attained slightly lower ultimate loads than did the corresponding Bresler-Scordelis beams. The ratio of the peak load of the Bresler-Scordelis beams to that of the Toronto beams (i.e., $P_{u,exp-BS} / P_{u,exp-VS}$) had a mean of 1.06 and a coefficient of variation of 5.1%. The Toronto beams generally experienced greater deflections at peak load than did the Bresler-Scordelis beams (see Figure 6(b)). The ratio of the deflection of the Bresler-Scordelis beams to that of the Toronto beams (i.e., $\delta_{u,exp-BS} / \delta_{u,exp-VS}$) had a mean of 0.75 and a coefficient of variation of 9.6%. The relatively flat

ultimate load plateau observed in some of the Toronto beams may account for some of the dissimilarity in results.

Detailed comparisons to the corresponding Bresler-Scordelis beams are made in Vecchio and Shim (2004), with discussion given to possible factors contributing to the differences observed.

FINITE ELEMENT ANALYSIS

Two-dimensional nonlinear finite element analyses were undertaken for each of the two sets of test beams. The analyses were performed using program VecTor2, developed at the University of Toronto and incorporating the behaviour models and constitutive relations of the Disturbed Stress Field Model (DSFM) (Vecchio, 2000; Vecchio, 2001). The DSFM is an extension of the Modified Compression Field Theory (MCFT) (Vecchio and Collins, 1986), and hence is a smeared rotating crack model. Principal to the formulation is the consideration of compression softening effects in the concrete due to transverse cracking, and of tension stiffening effects due to bond mechanisms between the concrete and the reinforcement. The DSFM, unlike the MCFT, also considers divergence of principal stress and principal strain directions, and takes into account slip deformations on crack surfaces.

The typical finite element meshes used to represent the Toronto beams are shown in Figure 7; meshes of 15 x 46, 15 x 56, and 15 x 66 eight-degree-of-freedom rectangular elements were used for the 4.1 m, 5.0 m and 6.8 m beams, respectively. Longitudinal reinforcement was modelled using truss bar elements; stirrup steel was modelled as smeared reinforcement. The steel loading plate, support plates, and rebar anchor plates were also simulated in the finite element representation. To model out-of-plane confinement effects in the concrete under the centre loading plate, out-of-plane reinforcement was added to the neighbouring elements; $\rho_z = 5\%$ was used for the two elements directly beneath the plate, and $\rho_z = 2.5\%$ was added to the ten elements adjacent to those two (see Figure 9). [As considered in VecTor2, the influence of the out-of-plane reinforcement results in some strength enhancement but, more importantly, considerable ductility enhancement.] The concrete and reinforcement material properties used were as previously reported in the details of the test specimens, except for the tensile strength of concrete which was estimated from the compressive strength as $0.33\sqrt{f'_c}$ (MPa). All constitutive modelling was done according to the default models of the DSFM. Loading was applied in a displacement-control mode (i.e., imposed midspan deflection) with a typical step size of 0.25 mm for the 4.1 and 5.0 m beams, and 0.50 mm for the 6.8 m beams.

The ultimate strengths calculated from the finite element analyses are compared to experimental results in Table 4; calculated load-deflection responses for the Toronto beams are compared to the measured responses in Figure 5. It is seen that reasonably accurate simulations of strength and load-deformation response were obtained. For the combined set of 24 beams, the ratio of the experimental-to-calculated strength ($P_{u,exp}/P_{u,calc}$) had a mean of 1.07 and a coefficient of variation of 12.0%. Interestingly, the

strengths of the Bresler-Scordelis beams were typically slightly under-estimated, while those of the Toronto beams were slightly over-estimated. The calculated load-deflection responses for the Toronto beams were somewhat over-estimated in terms of stiffness, falling closer to the observed responses of the Bresler-Scordelis beams. Displacements at ultimate load were generally under-estimated (see Table 4). In all cases, the correct modes of failure were calculated. Crack patterns were also in reasonably good agreement with test observations.

Of particular interest here is the degree to which the post-peak ductility of the test beams was captured by the nonlinear finite element. As evident from Figure 5, the calculated responses for beams containing web reinforcement typically showed less post-peak deflection capacity than did the experimental results. It is not known to what extent this under-estimate of ductility is associated with difficulties relating to the modelling of the concrete crushing near the load application point; more thorough experimental investigation is required. In beams containing no web reinforcement, the absence of any post-peak ductility was correctly modelled.

CASE STUDY

Shown in Figure 8 is a reinforced concrete industrial structure comprised of a single-bay seven-storey moment resisting frame. The structure was recently built in a high seismic zone region (with a 7.0 Richter magnitude earthquake as the design condition). The L-shaped columns of the structure, with a total depth of 2.7 m, are heavily reinforced in the vertical direction and contain an adequate amount of tie reinforcement (see Figure 9). Shown in Figure 10 are details of a typical beam. This particular beam, located at the second floor level, contains 28 #10 top bars and 26 #10 bottom bars with each set of bars continuous along the entire length of the beam. As well, 14 #6 horizontal bars, located in the mid-depth regions of the beam, are provided for crack control. The shear reinforcement consists of #4 double stirrups spaced at 150 mm, giving a shear reinforcement ratio of approximately 0.4%.

A subsequent review of the design indicated three distinct violations of the provisions specified in Chapter 21 of the ACI Code (ACI 318), as it relates to seismic detailing of moment resisting frames. They are:

- i) The span-to-depth ratio of the beam, at 3.8, is less than the required 4.0. Thus, it is expected that the shear stress demand on the beam will be high.
- ii) The beam longitudinal reinforcement terminates before entering the core of the column, as opposed to the required detail where the reinforcement is continuous through the core and hooked into the outside layer of the column reinforcement. This detail could result in bond failure of the beam reinforcement, or in vertical splitting of the joint or column due to inadequate tension force capacity.
- iii) Most importantly, the calculated shear capacity of the beam is not sufficient to allow the full flexural load capacity to be realized. Hence, the beams are shear-critical.

A finite element model, for VecTor2 analysis, was constructed to represent a typical beam-column joint in the structure. The mesh shown in Figure 11 consisted of 1022 rectangular elements and 184 truss elements, representing the joint at the second-storey level. The in-framing beam was modelled to the midspan and the in-framing columns were modelled to approximately the mid-storey heights above and below.

The beam's top and bottom longitudinal reinforcement were modelled as discrete bar layers using the truss bar elements (provided in one layer, both top and bottom), with the location of the bar layers consistent with the centroid of the reinforcing bars. The beam's shear and skin reinforcement, and all vertical and tie reinforcement in both the column and joint, were represented as smeared. To explicitly model bond stresses and bond slip in the beam's longitudinal reinforcement, contact elements were used to connect between the rectangular elements (concrete) and the truss bar elements (reinforcement) in the joint region.

Under seismic load conditions, the components of a structure, and the joints in particular, are required to exhibit strong measures of ductility in order to ensure adequate energy dissipation within the structure. A generally accepted criterion amongst jurisdictions and code authorities for assessing adequate ductile behaviour does not exist, although many are incorporating criteria based on the concept of displacement or ductility demand. The New Zealand criterion, for example, states that if the structure can withstand four cycles at four times the yield displacement with no more than a 20% decay in force capacity, then it is adequately designed to resist high seismic loading. It is understood at the outset that this is a highly stringent criterion, particularly when isolating the behaviour at a single beam-column joint. Given the size and nature of the structure being considered here, the ability to withstand four cycles at a displacement amplitude of three times the yield displacement would have been considered adequate evidence of good ductile behaviour.

In a preliminary analysis, it was determined that the first yielding of the reinforcement in the beam (i.e., of the top bars of the beam at the column face) occurs at a positive (downward) displacement of 30 mm at the beam tip (i.e., at the midspan). Hence, an analysis was undertaken wherein the beam tip was to be subjected to four cycles at plus/minus three times yield displacement (i.e., 4 cycles of +/- 90 mm). For this analysis, a constant axial stress of 3.0 MPa was assumed to be present in the column, reflecting in-service gravity load conditions.

The structure was not able to withstand the four cycles of three times yield displacement. During the first excursion to +90 mm, the beam sustained an interface shear failure at the column face at a displacement level of 45 mm (i.e., at 1.5 times yield displacement). The calculated load-deflection plot, shown in Figure 12, indicates a sudden failure with complete loss of load capacity. Figures 13(a) and 13(b) show the crack and displacement conditions at the yield load and immediately prior to failure, respectively.

Prior to failure, there was no evidence of any distress relating to column splitting or joint shear. Also, there was no indication from the analysis results that bond slip was occurring in the anchorage zone of the beam reinforcement. Hence, the amount of column tie reinforcement provided was sufficient to avert all distress mechanisms relating to the beam reinforcement anchorage detail. Rather, the low span-to-depth ratio of the beam, and the relatively low amount of shear reinforcement provided, predisposed the beam to the prospect of a shear-related mechanism controlling the behaviour. Significant web (diagonal) shear distress was evident in the beam prior to the failure, suggesting that a web shear failure was imminent (see Figure 13). First yielding of the beam stirrups occurred at a beam displacement of 26 mm (i.e., prior to flexural yielding) and quickly spread over large sections of the beam. The width of the web shear cracks ranged from 1.5 mm to 2.0 mm; shear cracks with widths of this magnitude are usually indicative of distress.

The web shear capacity of the beam was checked according to American Concrete Institute Standard ACI-318-99 (Clause 11.3). Using unfactored material properties, a web shear resistance of 4960 kN was calculated. The beam tip load at the time of the interface failure (i.e., the flexural yield load) was 5040 kN. Hence, the web shear capacity of the beam is fully exhausted, according to code strength calculations, before flexural hinging can occur. Further, it should be noted that the code formulation was not meant to address situations in which the element is subjected to reversed cyclic shear. Under load reversal, a second and roughly perpendicular set of diagonal shear cracks will develop in the beam, further weakening the shear resistance. It is most likely that under these conditions, a web shear failure will occur at displacement levels lower than the yield displacement for this beam.

One option open to the designers, in lieu of satisfying the requirements of ACI-318 Chapter 21, is to model the entire structure and subject it to a push-over analysis. Here, lateral displacements corresponding to a specified level of drift would be applied in increments, and the structure would be required to withstand these without collapse. As demonstrated in Figure 14, in such an analysis, a well-designed structure will be governed by flexural hinging at the joints, thus allowing high levels of ductility to be achieved. An 'unacceptable' situation exists if the shear capacity of the members is exhausted before flexural hinging and before sufficient lateral displacement is attained. The structure in question likely lies in the latter category. Whether sufficient lateral deformability can be demonstrated, and if so whether it is an accurate representation of true structural behaviour, will depend largely on how well the post-peak shear ductility is modelled in the analysis program. Hence, the need exists for accurate analytical models to properly represent this mechanism.

CONCLUSIONS

From the experimental and analytical investigations undertaken, the following conclusions can be drawn:

1. The test results of the classic series of beams tested by Bresler and Scordelis were largely reproducible.
2. In the test beams containing no web reinforcement, sudden and brittle failures were brought on by the formation of a critical diagonal tension crack extending into a longitudinal splitting crack through to the end of the beam. In these shear-critical beams, no ductility existed beyond the peak load point.
3. In the test beams containing web reinforcement (up to 0.2 %), somewhat more ductile flexural-shear failures developed with the crushing, splitting and spalling of concrete in the flexural compression zone and beneath and adjacent to the central loading plate. Shear mechanisms played a significant role in the behaviour of the short- and intermediate-length specimens. In all cases, deformation capacity beyond the peak load was present but limited.
4. Nonlinear finite element analyses were reasonably accurate in reproducing aspects of behaviour such as peak load capacity, load-deformation response prior to peak, cracking patterns, rebar stresses and failure modes.
5. Simulations of the post-peak response were only marginally well reproduced. Additional experimental and analytical work is required to improve capabilities in this regard.
6. As demonstrated by the case study, practical situations can arise in which accurate tools for assessing the post-peak ductility of shear-critical members are required.

REFERENCES

- Bresler, B. and Scordelis, A.C., 1963, "Shear strength of reinforced concrete beams," *Journal of American Concrete Institute*, V. 60, No. 1, pp. 51-72.
- Vecchio, F.J., 2000, "Disturbed stress field model for reinforced concrete: Formulation," *ASCE Journal of Structural Engineering*, V. 126, No. 9, pp. 1070-1077.
- Vecchio, F.J., 2001, "Disturbed stress field model for reinforced concrete: Implementation," *ASCE Journal of Structural Engineering*, V. 127, No. 1, pp. 12-20.
- Vecchio, F.J. and Collins, M.P., 1986, "The modified compression field theory for reinforced concrete elements subjected to shear," *Journal of American Concrete Institute*, V. 83, No. 2, pp. 219-231.
- Vecchio, F.J. and Shim, W., 2004, "Experimental and analytical re-examination of classic concrete beam tests," *ASCE Journal of Structural Engineering*, V. 130, No. 3, pp. 460-469.

Table 1 - Test Beam Details.

Beam No.	b (mm)	h (mm)	d (mm)	L (mm)	Span (mm)	Bottom Steel	Top Steel	Stirrups
OA1	305	552	457	4100	3660	2 M30, 2 M25	-	-
OA2	305	552	457	5010	4570	3 M30, 2 M25	-	-
OA3	305	552	457	6840	6400	4 M30, 2 M25	-	-
A1	305	552	457	4100	3660	2 M30, 2 M25	3 M10	D5 @ 210
A2	305	552	457	5010	4570	3 M30, 2 M25	3 M10	D5 @ 210
A3	305	552	457	6840	6400	4 M30, 2 M25	3 M10	D4 @ 168
B1	229	552	457	4100	3660	2 M30, 2 M25	3 M10	D5 @ 190
B2	229	552	457	5010	4570	2 M30, 2 M25	3 M10	D5 @ 190
B3	229	552	457	6840	6400	3 M30, 2 M25	3 M10	D4 @ 152
C1	152	552	457	4100	3660	2 M30	3 M10	D5 @ 210
C2	152	552	457	5010	4570	2 M30, 2 M25	3 M10	D5 @ 210
C3	152	552	457	6840	6400	2 M30, 2 M25	3 M10	D4 @ 168

Table 2 - Material Properties

Bar Size	Reinforcement				
	Diameter (mm)	Area (mm ²)	f_y (MPa)	f_u (MPa)	E_s (MPa)
M10	11.3	100	315	460	200000
M25*	25.2	500	440	615	210000
M25**	25.2	500	445	680	220000
M30	29.9	700	436	700	200000
D4	3.7	25.7	600	651	200000
D5	6.4	32.2	600	649	200000

*Series 2 **Series 1 and 3

Beam No.	Concrete			
	f'_c (MPa)	ϵ_o (mm/mm)	E_c (MPa)	f_{sp} (MPa)
OA1	22.6	0.0016	36500	2.37
OA2	25.9	0.0021	32900	3.37
OA3	43.5	0.0019	34300	3.13
A1	22.6	0.0016	36500	2.37
A2	25.9	0.0021	32900	3.37
A3	43.5	0.0019	34300	3.13
B1	22.6	0.0016	36500	2.37
B2	25.9	0.0021	32900	3.37
B3	43.5	0.0019	34300	3.13
C1	22.6	0.0016	36500	2.37
C2	25.9	0.0021	32900	3.37
C3	43.5	0.0019	34300	3.13

Table 3 - Comparison of details between Toronto Beams and Bresler-Scordelis Beams

Beam No.	Concrete			Transverse Reinforcement			Tension Reinforcement			Compression Reinforcement		
	f'_{c-BS}	f'_{c-VS}	$\frac{f'_{c-BS}}{f'_{c-VS}}$	ρ_{v-BS}	ρ_{v-VS}	$\frac{\rho_{v-BS}}{\rho_{v-VS}}$	A_{s-BS}	A_{s-VS}	$\frac{A_{s-BS}}{A_{s-VS}}$	A'_{s-BS}	A'_{s-VS}	$\frac{A'_{s-BS}}{A'_{s-VS}}$
	(MPa)	(MPa)		(%)	(%)		(mm ²)	(mm ²)		(mm ²)	(mm ²)	
OA1	22.6	22.6	1.00	-	-	-	2579	2400	1.07	253	300	0.84
OA2	23.7	25.9	0.92	-	-	-	3224	3100	1.04	253	300	0.84
OA3	37.6	43.5	0.86	-	-	-	3868	3800	1.02	253	300	0.84
A1	24.1	22.6	1.07	0.100	0.100	1.00	2579	2400	1.07	253	300	0.84
A2	24.3	25.9	0.94	0.100	0.100	1.00	3224	3100	1.04	253	300	0.84
A3	35.1	43.5	0.81	0.100	0.100	1.00	3868	3800	1.02	253	300	0.84
B1	24.8	22.6	1.10	0.148	0.148	1.00	2579	2400	1.07	253	300	0.84
B2	23.2	25.9	0.90	0.148	0.148	1.00	2579	2400	1.07	253	300	0.84
B3	38.8	43.5	0.89	0.148	0.147	1.00	3224	3100	1.04	253	300	0.84
C1	29.6	22.6	1.31	0.202	0.202	1.00	1289	1400	0.92	253	300	0.84
C2	23.8	25.9	0.92	0.202	0.202	1.00	2579	2400	1.07	253	300	0.84
C3	35.1	43.5	0.81	0.202	0.201	1.00	2579	2400	1.07	253	300	0.84
Mean			0.96			1.00			1.04			0.84

Table 4 - Comparison of Observed and Calculated Results.

Beam No.	Ultimate Load			Midspan Deflection			Beam No.	Ultimate Load			Midspan Deflection		
	$\frac{P_{u-Test}}{P_{u-Calc}}$	$\frac{P_{u-Test}}{P_{u-Calc}}$	$\frac{P_{u-Test}}{P_{u-Calc}}$	$\frac{\delta_{u-Test}}{\delta_{u-Calc}}$	$\frac{\delta_{u-Test}}{\delta_{u-Calc}}$	$\frac{\delta_{u-Test}}{\delta_{u-Calc}}$		$\frac{P_{u-Test}}{P_{u-Calc}}$	$\frac{P_{u-Test}}{P_{u-Calc}}$	$\frac{P_{u-Test}}{P_{u-Calc}}$	$\frac{\delta_{u-Test}}{\delta_{u-Calc}}$	$\frac{\delta_{u-Test}}{\delta_{u-Calc}}$	$\frac{\delta_{u-Test}}{\delta_{u-Calc}}$
	(kN)	(kN)		(mm)	(mm)		(kN)	(kN)		(mm)	(mm)		
BS-OA1	334	316	1.06	6.6	12.0	0.55	VS-OA1	331	311	1.06	9.1	9.5	0.96
BS-OA2	356	270	1.32	11.7	18.5	0.63	VS-OA2	320	287	1.11	13.2	12.8	1.03
BS-OA3	378	294	1.29	27.9	20.8	1.34	VS-OA3	385	333	1.16	32.4	25.5	1.27
BS-A1	468	472	0.99	14.2	15.8	0.90	VS-A1	459	476	0.96	18.8	14.3	1.31
BS-A2	490	399	1.23	22.9	19.5	1.17	VS-A2	439	457	0.96	29.1	21.8	1.33
BS-A3	468	366	1.28	35.8	44.6	0.80	VS-A3	420	447	0.94	51.0	51.3	0.99
BS-B1	446	423	1.06	13.7	15.3	0.90	VS-B1	434	423	1.03	22.0	15.8	1.39
BS-B2	400	327	1.22	20.8	19.5	1.07	VS-B2	365	384	0.95	31.6	22.3	1.42
BS-B3	356	355	1.00	35.3	39.0	0.91	VS-B3	342	376	0.91	59.6	51.2	1.16
BS-C1	312	307	1.02	17.8	18.3	0.97	VS-C1	282	289	0.98	21.0	15.3	1.37
BS-C2	324	258	1.26	20.1	17.3	1.16	VS-C2	290	306	0.95	25.7	20.6	1.25
BS-C3	270	255	1.06	36.8	36.3	1.01	VS-C3	265	283	0.94	44.3	43.2	1.03
BS Series	Mean	1.15		Mean	0.95		VS Series	Mean	1.00		Mean	1.21	
	COV (%)	11.04		COV (%)	23.65			COV (%)	7.78		COV (%)	13.93	
BS and VS series								Mean	1.07		Mean	1.08	
								COV (%)	12.03		COV (%)	21.76	

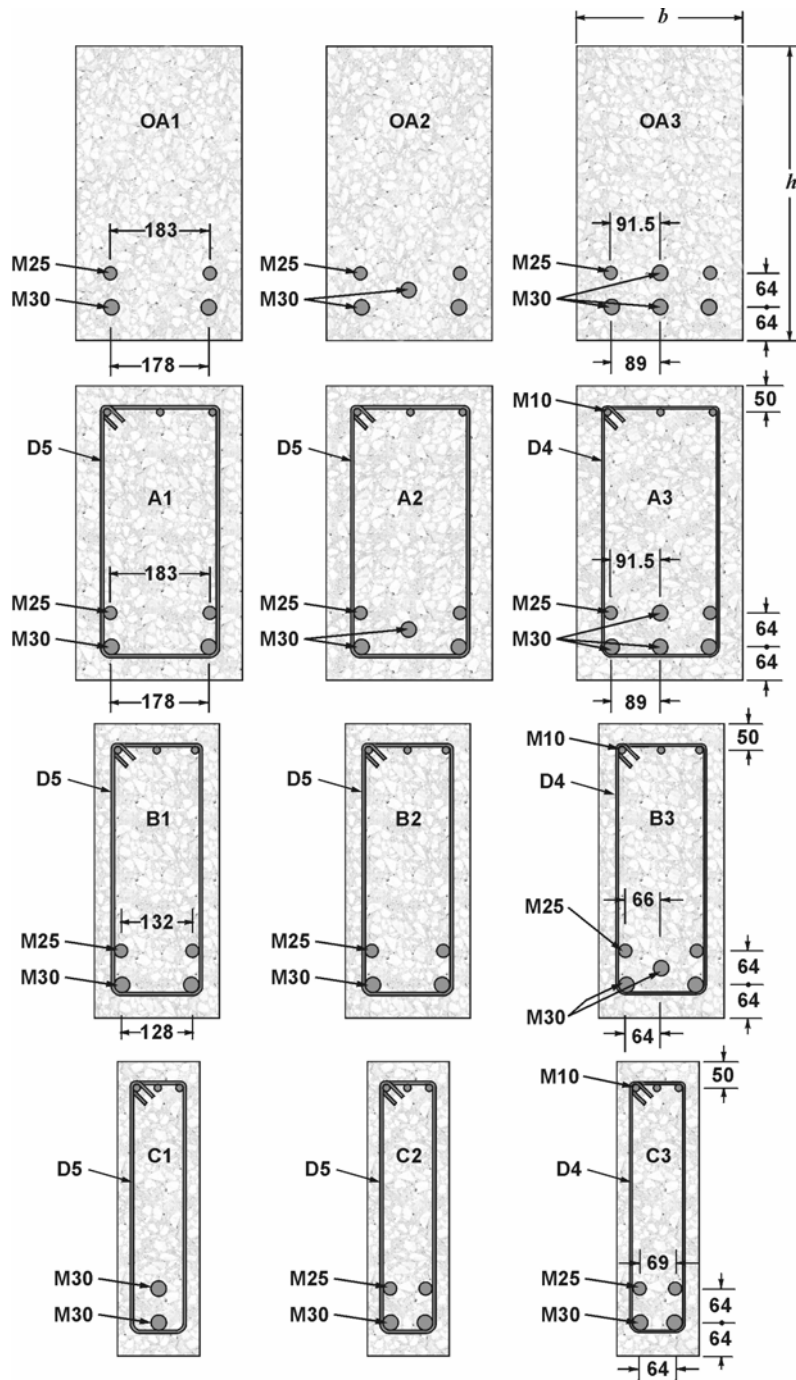


Figure 1 - Cross section details of Toronto Beams.

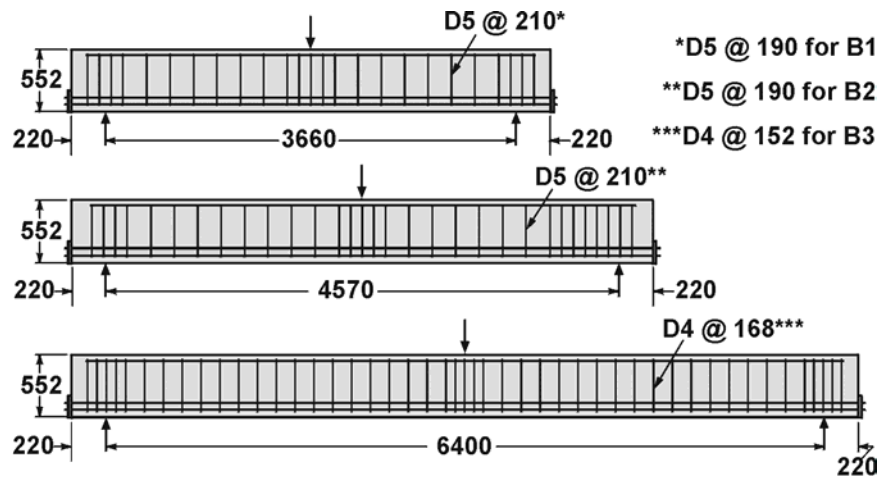


Figure 2 - Profile details of Toronto Beams.

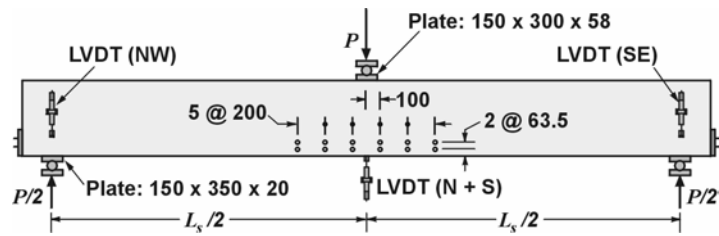
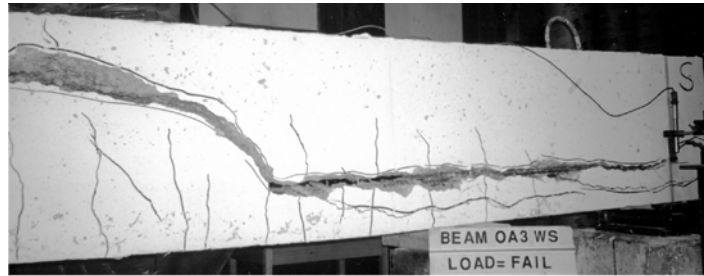
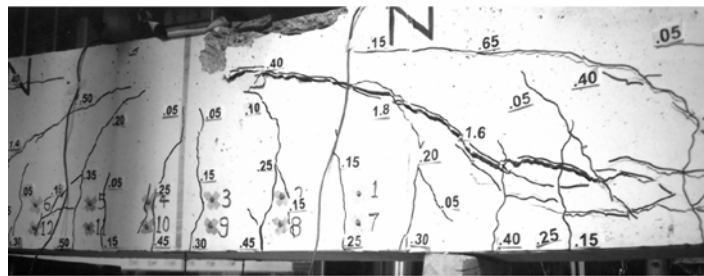


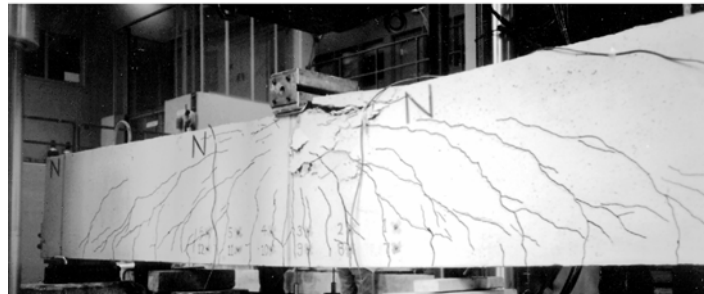
Figure 3 - Test set-up.



(a) VS-OA3



(b) VS-A1



(c) VS-B1

Figure 4 - Photos of test beams. (a) Beam VS-OA3. (b) Beam VS-A1. (c) Beam VS-B1

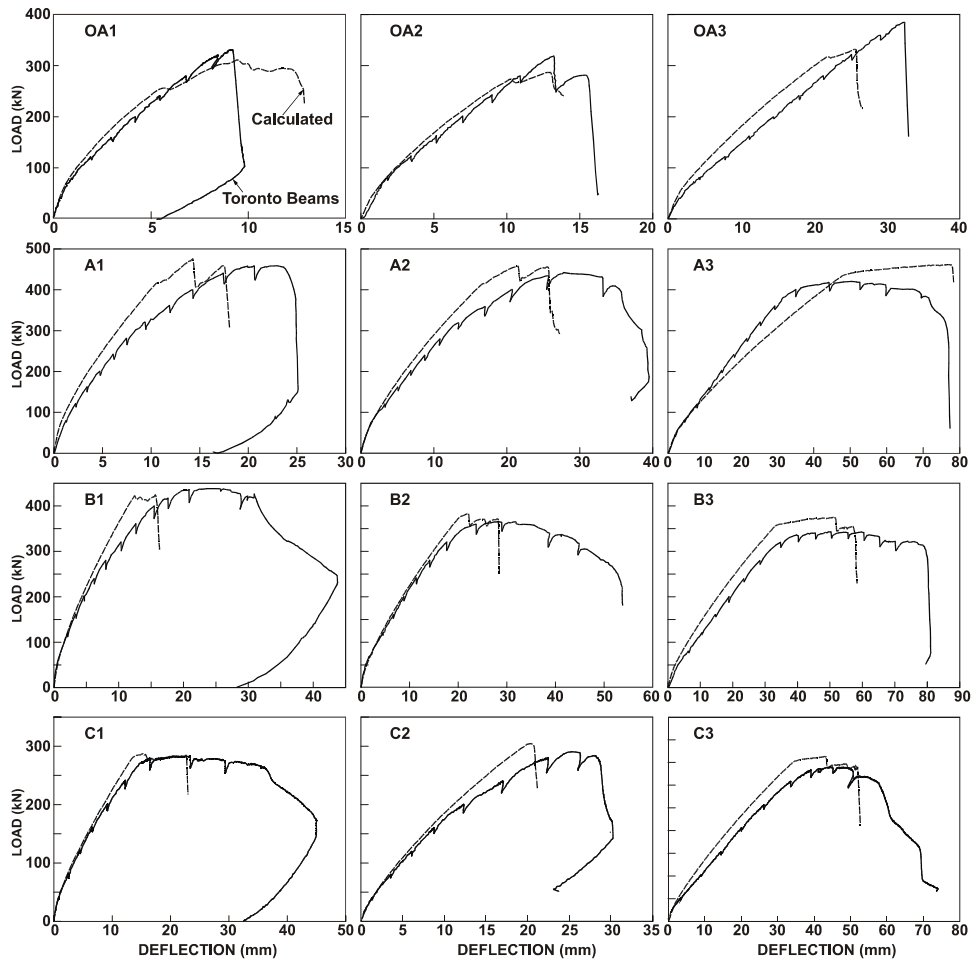


Figure 5 - Observed and calculated load-deflection responses for Toronto Beams.

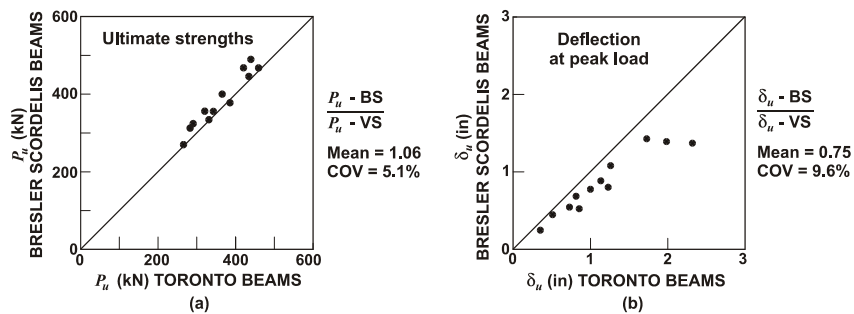


Figure 6 - Comparison of results to Bresler-Scordelis beams.

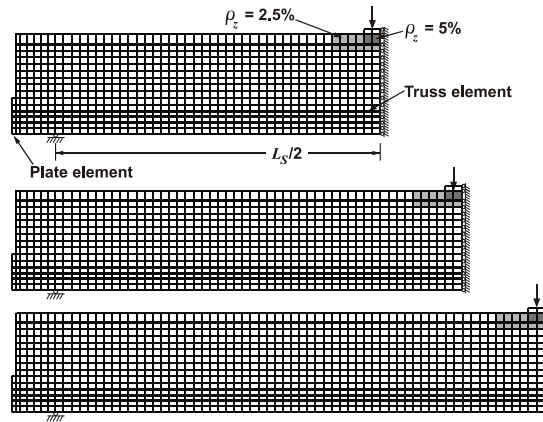


Figure 7 - Finite element meshes for test beams.

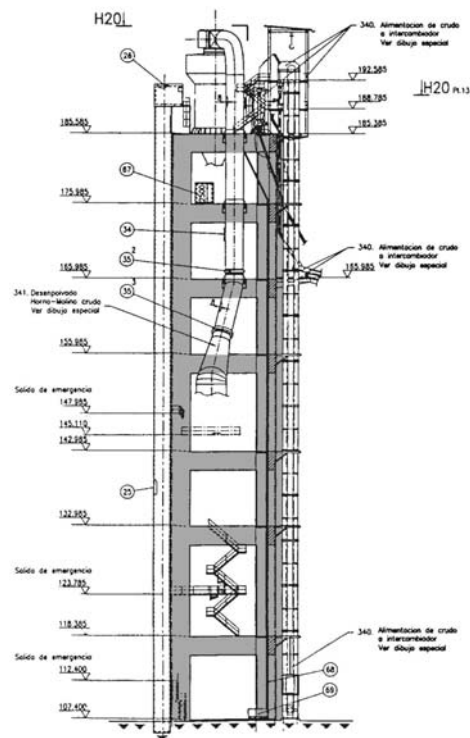


Figure 8 - Elevation details of industrial structure designed for earthquake zone.

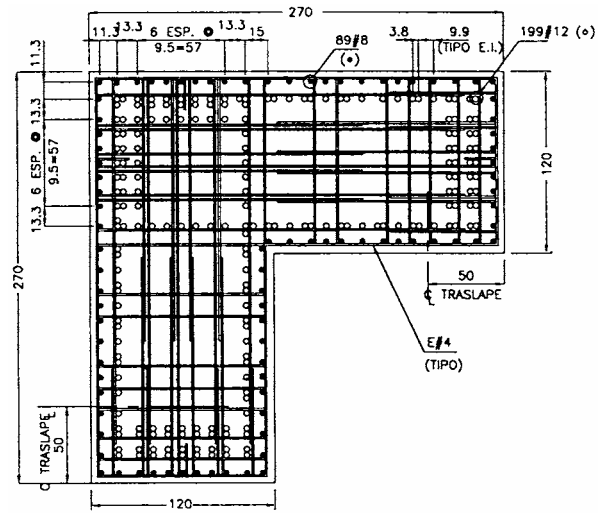


Figure 9 - Typical column details (Note: dimensions are in cm).

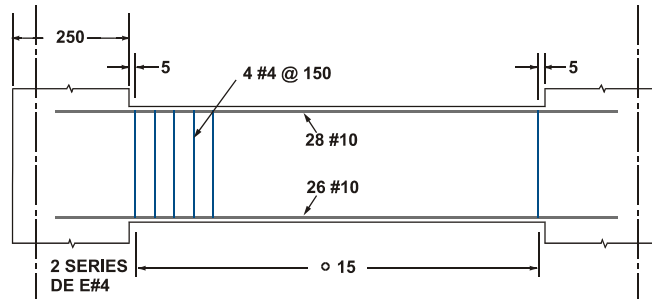


Figure 10 - Typical beam details.

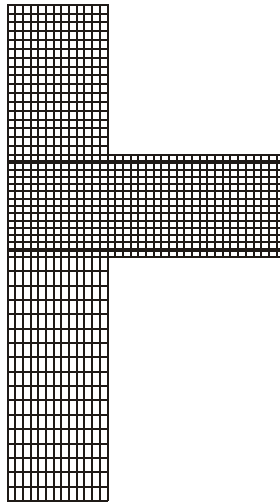


Figure 11 - Finite element model for typical beam-column joint

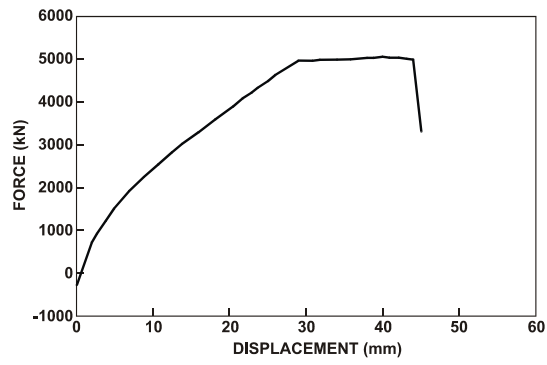


Figure 12 - Calculated load-deflection response of beam-column assembly.

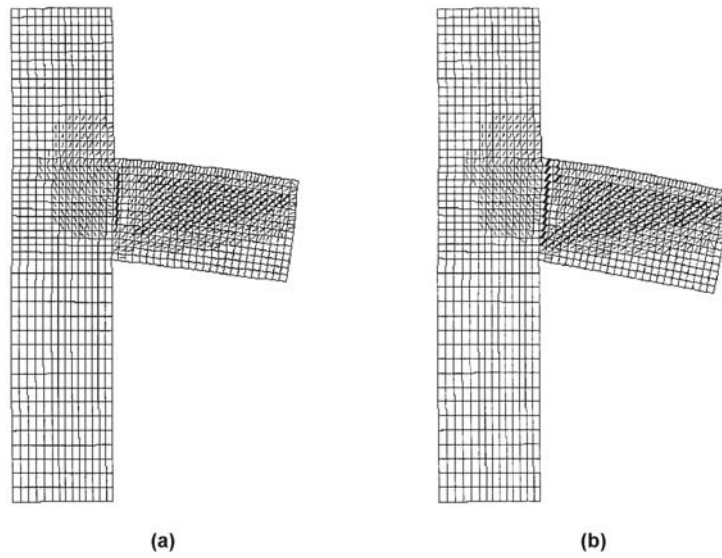


Figure 13 - Crack and damage patterns. (a) At first yield. (b) Immediately prior to failure.

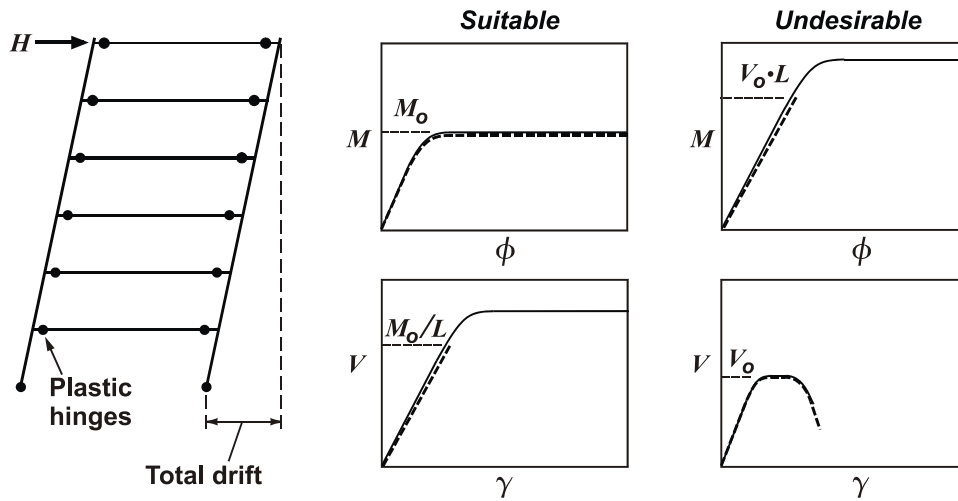


Figure 14 - Push-over analyses of frames.